Proc. 25th Winter Workshop on Nuclear Dynamics (2009) 000–000

25th Winter Workshop on Nuclear Dynamics
Big Sky, Montana, USA
February 1–8, 2009

A FOrward CALorimeter (FOCAL) for PHENIX

Richard Seto[1] for the PHENIX collaboration

[1] University of California, Riverside,
92521 Riverside, CA, USA

Abstract. This article describes a proposed new calorimeter which covers a rapidity of $1 < |\eta| < 3$ increasing the acceptance of the PHENIX detector for photons by more than a factor of 10. This will extend photon measurements into a region probing the lox-x portion of the nucleus, which will give clean measurements of ΔG in the proton, measurements of various transverse spin structure functions such as the Sivers effect, and of the nuclear gluon structure functions, crtical for understanding heavy ion collisions.

Keywords: calorimeter, RHIC, PHENIX, gluon, spin, photon, QGP, QCD
PACS: 21.65.Qr, 24.87.+y, 25.75.-q, 29.40.Vj, 29.40.Gx

1. Introduction

Physics requiring a large rapidity coverage for photons and jets has taken center stage in the RHIC program, hence a calorimeter covering several units of rapidity with full azimuthal coverage is crucial to the PHENIX experiment. Together with the present PHENIX detector and the addition of the the high granularity silicon detectors, the FOrward Calorimeter (FOCAL) will give PHENIX the capability to measure photons and jets over the range $-4 < \eta < 4$ giving us access to kinematic variables, in particular Bjorken x, in p+p and d+Au collisions. It will also vastly increase the capability to measure direct photons in heavy ion collisions. The proposed FOCAL detector has 4 primary physics goals which are summed up clearly in the milestones set forth by the Nuclear Science Advisory Committee (NSAC) [1]. These are:

- DM8: Determine gluon densities at low x in cold nuclei via p+ Au or d + Au collisions
- HP12: Utilize polarized proton collisions at center of mass energies of 200 and 500 GeV, in combination with global QCD analysis, to determine if gluons

have appreciable polarization over any range of momentum fraction between 1 and 30% of the momentum of a polarized proton.

- DM10: Measure jet and photon production and their correlations in A200 ion+ion collisions at energies from medium RHIC energies to the highest achievable energies at LHC. DM10 captures efforts to measure jet correlations over a span of energies at RHIC and a new program using the CERN Large Hadron Collider and its ALICE, ATLAS and CMS detectors.

- HP13: Test unique QCD predictions for relation between single-transverse spin phenomena in p-p scattering and those observed in deep-inelastic lepton scattering. New Milestone HP13 reflects the intense activity and theoretical breakthroughs of recent years in understanding the parton distribution functions accessed in spin asymmetries for hard-scattering reactions involving a transversely polarized proton. This leads to new experimental opportunities to test all our concepts for analyzing hard scattering with perturbative QCD.

The FOCAL detector is extremely compact since it is composed of layers of tungsten interleaved with silicon pads for readout. The pads are 1.55x1.55 cm^2, and will be read out in 3 longitudinal segments in depth for the separation of hadronic and electromagnetic showers[2]. To increase the capability of identifying photons and π^0's, the front portion of the detector is instrumented with 0.5 mm silicon strips, thereby giving a two track separation capability of a few mm or about 10 mr, for collisions at the nominal vertex point. This makes possible the measurement of π^0's up to an energy of greater than 50 GeV.

One of the important new avenues of study that will become accessible with the FOCAL, is the study of transverse spin physics and associated questions - in particular, the possibility that such studies may shed light on the portion of the proton spin carried by the parton angular momentum. While simulations of the relevant signatures are at a early stage, the study of transverse spin effects is a major new area of physics which the FOCAL will make possible.

2. Design

The FOCAL detector is located about 40 cm from the nominal vertex position on the front pole-tips of the muon magnets. For ease of construction and maintenance it will be composed of "bricks" stacked up in a circular shape as shown in Fig. 1 and will be supported on a structure mounted on the pole-tip. Each brick is composed of silicon tungsten sandwich towers - 4mm tungsten interleaved with 1.55x1.55 cm^2 silicon pads. The analog signals from the pads are passively summed together in 3 longitudinal segments, EM0, EM1 and EM2, passed through a pre-amplifier and read out by a 50 MHz 14 bit ADC (Fig. 1, bottom). The total depth of the calorimeter is about 24 radiation lengths. The EM0 section has an an additional component - 4 sets of x-y silicon strip detectors with a pitch of 0.5 mm as shown in

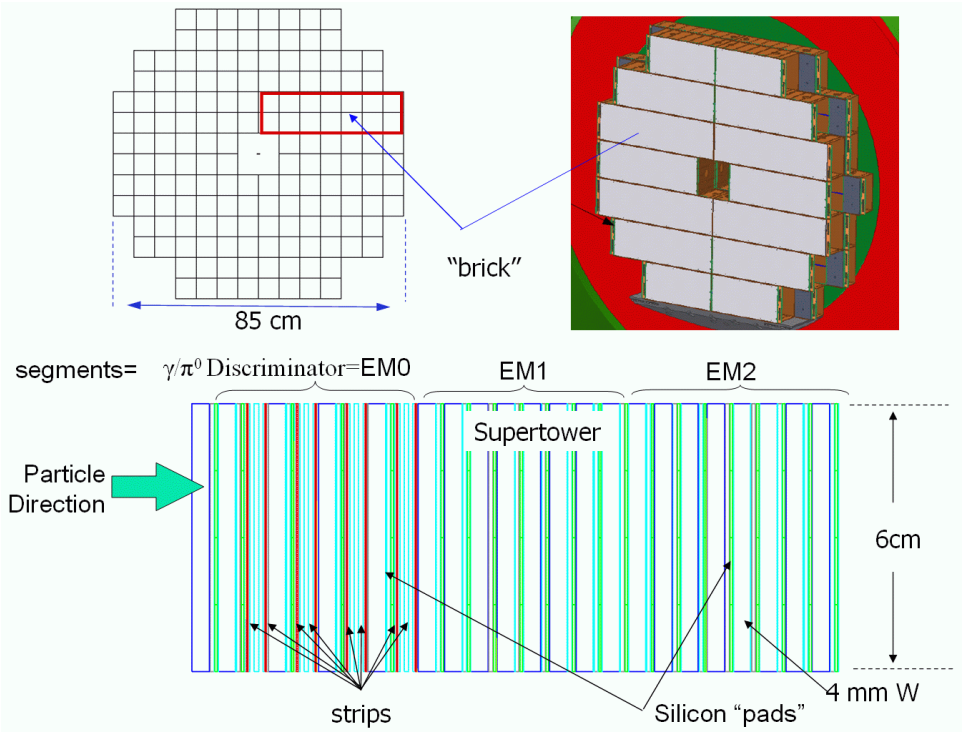

Fig. 1. The mechanical design of the FOCAL. The device is built from "bricks" which are stacked on a support stand on the pole-tips of the PHENIX muon magnets (top-right). Each brick is composed of between 8 and 14 "super-towers." Each supertower (bottom) is a silicon-tungsten sandwich composed of silicon layers divided into 16 1.5x1.5 cm^2 pads/layer, and 4mm thick tungsten plates . The structure is read out in 3 longitudinal segments, EM0, EM1 and EM2. In addition EM0 is augmented with 4 x-y planes of 0.5 mm strips read out individually for the reconstruction of overlapping showers as explained in the text.

the figure. Each strip detector is 6.2x6.2 cm^2 and is read out using the 8 bit SVX-4 chip developed for the CDF/D0 detectors at FNAL.

3. How it works

Since the calorimeter is close to the vertex and has large coverage, particles will enter the detector at a variety of angles. The FOCAL will track particles in the same way that a standard multi-plane tracking device would handle the problem. Shower candidates are found in each of the EM0, EM1, and EM2 segments individually

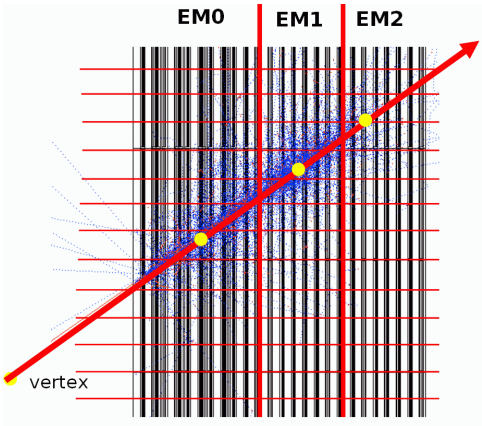

Figure 2 A section of the FOCAL, showing the reconstruction of a large angle track. Clusters are formed in the segments, EM0, EM1 and EM2. Each "hit" is the center of gravity of the clusters. Additional points will come from the strip detectors, and by assuming the vertex. An iterative pattern recognition algorithm uses a parametrization of the shower shape for energy sharing among the clusters in a segment and among the tracks in the calorimeter.

and the center of gravity of the shower is designated as a hit. Together with the vertex, and hits in the strip planes, straight shower "tracks" can be formed. The question of projective geometry is circumvented by allowing showers to be formed from segments which can be at a large angle (see Fig. 2). Once showers have been formed, particle identification algorithms are applied to differentiate between electromagnetic and hadronic particles.

Showers from high energy π^0s will overlap and can be mis-identified as single photons. The strip detectors will allow π^0's up to about 60 GeV in energy to be identified. The left-hand figure of Fig. 3, left shows a 50 GeV π^0 where the two showers overlap one another in the calorimeter. The middle two figures show the same event in an expanded x and y view showing the hits on the strip detectors. One can clearly see the photon conversions to a dielectron pairs which can then be reconstructed as two separate tracks. Note that there is no magnetic field in the calorimeter, hence the electron and positron do not open up and each converted photon will be seen a single 2 MIP track in the strip detectors. This will then give an opening angle for the π^0. The total energy is given by the pad information. Two methods can be used to find the energy asymmetry. The first and simplest is to simply divide the energy into two equal pieces; the second option is to use the asymmetry measured by the strips since the SVX-4 measures a charge, as a rough estimation of the energy division. Fig. 3, right shows an example where we use the former method. In the simulation, photons and π^0's are embedded into a p+p minimum bias event. The figures show the invariant mass distribution reconstructed in the case where 10 GeV π^0's are embedded (top-right) and 10 GeV photons are embedded. The plots include only those events in which the shower finding algorithm found only one of the showers or the showers overlap and were identified as one electro-magnetic shower. Asymmetric events in which two-photons were found at a large enough separation are handled in the standard 2-track method of reconstruction. Those in this plot are designated as "single-track" π^0 candidates.

The top-right plot shows a nice π^0 peak at the correct mass In the case when two tracks are found for a single photon by the strip detectors, the mass reconstructs to low energy allowing for a γ/π^0 separation. In a sample where we have optimized our cuts for a minimum of π^0's to be mis-identified as photons we find the suppression factor for π^0's to be about a factor of 7 from 5 to 60 GeV energy. The suppression factor is the the efficiency for identifying real photons as photons divided by the probability for the misidentification of π^0s as photons. In simple terms this means that for overlapping showers (i.e. electromagnetic showers identified by the shower finding algorithm using the pad information) coming from π^0s, about 85% can be rejected. This together with other criteria such as isolation cuts, is sufficient for the measurement of direct photons.

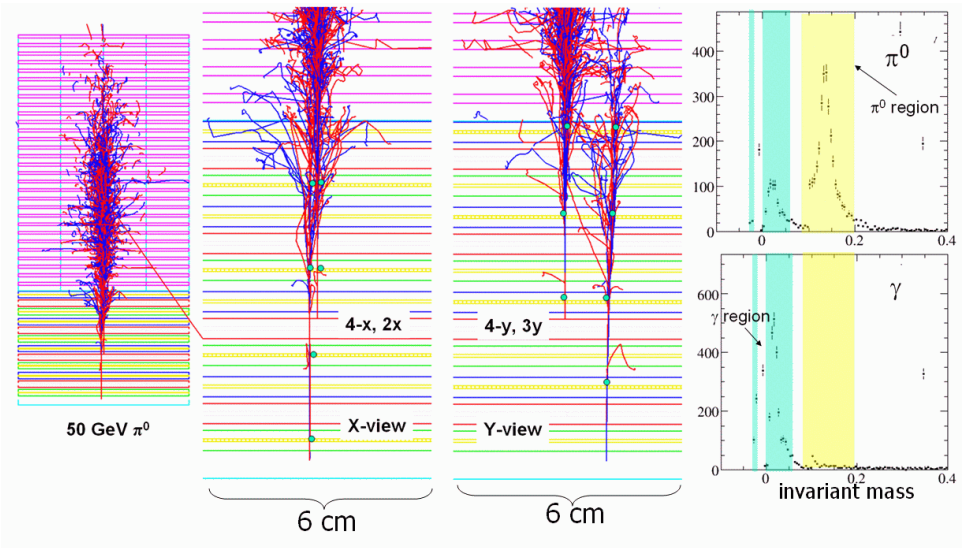

Fig. 3. Left: A 50 GeV π^0 in the FOCAL where the π^0 appears as one electromagnetic shower. Middle two plots: An greatly expanded view of the x and y views of the first segment (EM0) of the calorimeter showing the clearly separated hits in the x and y views allowing for the reconstruction of the π^0. Top-right: The reconstruction of 10 GeV π^0s embedded in a p+p event in the FOCAL. The π^0 peak shows up at the π^0 mass. Right, bottom: Same - except that the embedded particles are 10 GeV photons. Photons show up at low mass.

4. Capabilities

Full simulations are now in progress. Here I give examples of two measurements that the FOCAL will pursue - the measurement of ΔG and the measurement of the

nuclear gluon structure functions.

4.1. ΔG

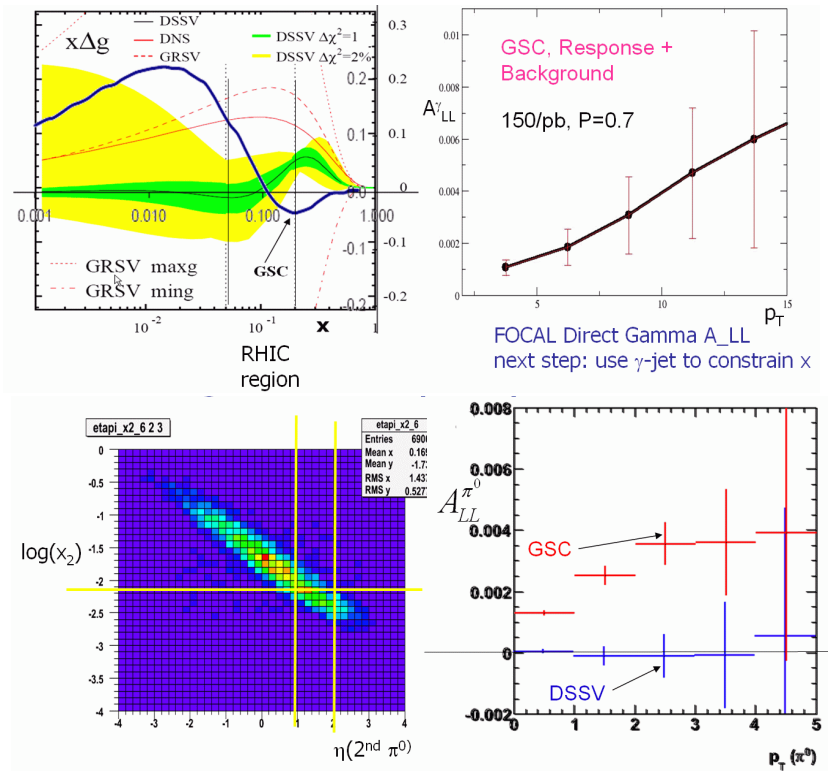

Fig. 4. Top left: $x\Delta g(x)$ from a fit to world's data (DSSV[3]) showing the large uncertainty in the low-x region. Also shown is the present region measured at RHIC at $x \sim 0.1$ and an example of a gluon structure function (GSC) which is consistent with present data and has a large contribution to ΔG. Note that the main contribution for GSC is at $x \sim 0.01$. Top right: Error bars from an inclusive direct γ measurement of $A_{LL}^{\pi^0}$ using the FOCAL. Bottom left: The correlation of η for a second π^0 and the x of the reaction for the $2\pi^0$ final state as explained in the text. Note that we can chose an η range of between 1 and 2 to select events with $x \sim 0.01$, where GSC is a maximum. Bottom right: The measurement of $A_{LL}^{\pi^0}$ where a selection of events has been done by choosing the range of η for the second π^0 as indicated in the left figure.

Present measurements of ΔG are consistent with zero, however this does not

necessarily mean that the spin contribution of the gluon to the proton is small. Fig. 4,top-left shows the present limits on ΔG which primarily come from measurements in the central rapidity region and probe $x \sim 0.1$. GSC[4] is an example of a distribution which would yield a small ΔG at $x \sim 0.1$, and yet would still imply that the gluon spin contribution is large - the majority of the contribution is at low x. In order to probe the low x region one must go to forward rapidities - a region covered by the FOCAL. Direct photons are a clean probe of the gluon spin, since they result primarily from a gluon-quark vertex, particularly at low x where the gluons are dominant. In addition one does not have to fold in a fragmentation function for the photon. In order to use inclusive direct photon measurement to measure ΔG one looks at the spin asymmetry of isolated direct photons. Even in the case of isolated electromagnetic clusters, there is a background which comes from isolated π^0's which are merged in the detector. One can use the technique described above to suppress this background. Using an algorithm which is tuned to give a clean direct photon signal, one is able to reduce the π^0 background by a factor of about 7, depending on the p_T. In the case of GSC this enables us to measure an asymmetry as shown in Fig. 4,top-right in a typical RHIC II run. The values of the asymmetry expected are extremely small - less than 0.005.

Now such a measurement still integrates over a rather large value of x. Measuring the photon plus the outgoing jet would allow us to select the particular value of x which we wish, in the case of GSC $x \sim 0.01$ where the contribution of the Gluon spin is the largest.

In this case what we have simulated the $2\pi^0$ signal which will have significantly more statistics than the γ+jet signal. One requires the highest p_T π^0 to have a p_T>2.5 GeV in the FOCAL. Looking azimuthally opposite this trigger π^0, one can then look at the distribution of the η of the opposing π^0 where there is a tight correlation between η and x_2 (Fig. 4, bottom-left). One can then look at the spin asymmetry. Fig. 4, bottom-right shows the measurement possible, again assuming a typical RHIC II run. It is compared with DSSV. The case of GSC and DSSV are clearly distinguishable. Note that the size of the asymmetry is still small. Picking a appropriate x value maximizes the asymmetry, but the fragmentation function dilutes it. The larger statistics, however works to our advantage. We are now studying the case of the gluon-jet final state where we select $x_2 \sim 0.01$ where the asymmetry should be much larger, albeit with smaller statistics.

4.2. Measuring Jets and x

In order to extract the Bjorken x of the parton using the well known relationship $x = \frac{p_T^\gamma}{\sqrt{(2)}}(e^{-y_\gamma} + e^{-y_{jet}})$ one will need to have a measurement of both the photon and the jet. The silicon vertex detector will allow the measurement of the jet within a rapidity of -1 to 1 while the FOCAL will allow us to extend this range to $1 < |\eta| < 3$ as well as measuring the photon. It is important to note that only the direction of the jet is needed. Fig. 5, bottom-left shows the jet angular resolution of the

FOCAL, leading to a resolution on x of about 15%. This then will further allow for an extraction of ΔG (simulations are not yet complete for this channel) and for the measurement of the nuclear gluon structure function in p+A(or d+A) collisions

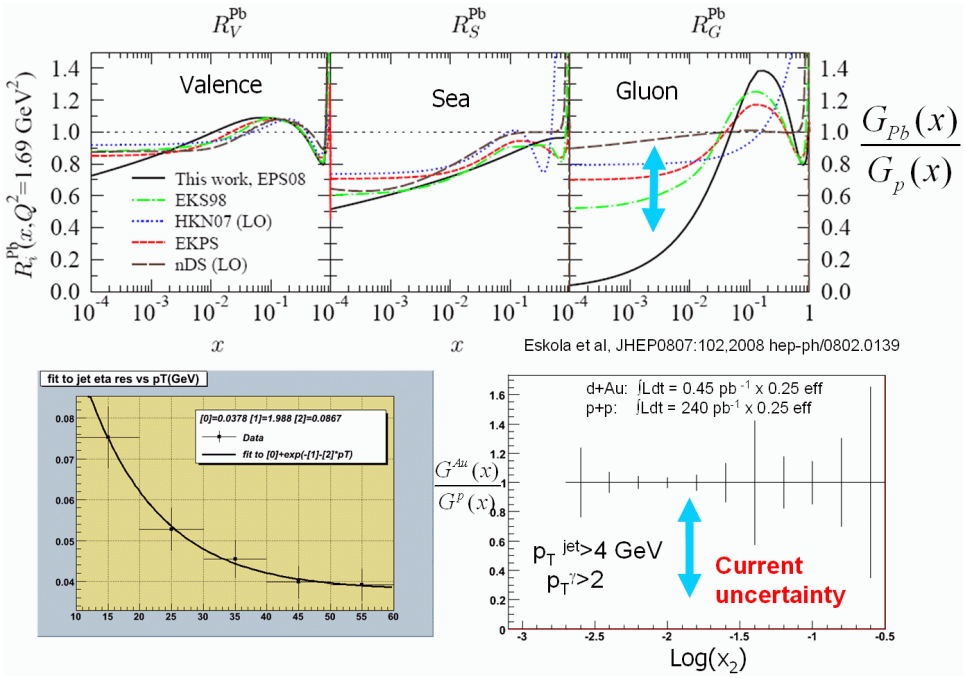

Fig. 5. Top: A variety of fits to world's data for structure functions in nuclei as compared to those in the proton[6][7]. Note that our knowledge of the gluon structure function at low x is very poor while that of the quarks is reasonably well known. Bottom left: The jet angular resolution measured by the FOCAL as a function of the transverse momentum of the jet. Right: The x_2 resolution resulting from the jet angular resolution in γ-jet events. Bottom right: The uncertainty in the nuclear gluon structure function from one run using the FOCAL - only statistics have been considered.

4.3. G_A, the nuclear gluon structure function

One of the crucial limitations to the predictive capability of hydrodynamic models of heavy ion collisions is the knowledge of the initial state gluon functionThe present knowledge of the gluon structure in nuclei is rather poor, particularly at low-x, the region important for the bulk particle production[6][7](Fig. 5, top). Direct photons presents a particularly clean channel in which to measure f_g^A the gluon structure

function in a nucleus A. The cross section can be written as

$$\frac{d^3\sigma}{dp_T^2 dy_\gamma dy_q} = x_1 f_g^p(x_1) F_{2A}(x_2, Q^2) \frac{\pi\alpha\alpha_S(Q^2)}{3\hat{s}^2} \left(\frac{1 + cos\theta^*}{2} + \frac{2}{1 + cos\theta^*} \right)$$
$$+ F_{2p}(x_1, Q^2) x_2 f_g^A(x_2) \frac{\pi\alpha\alpha_S(Q^2)}{3\hat{s}^2} \left(\frac{1 - cos\theta^*}{2} + \frac{2}{1 - cos\theta^*} \right)$$

The gluon and quark structure functions in the proton, f_g^p and F_{2p}, and the quark structure function in the nucleus F_{2A} (at least in some nuclei) are reasonably well known. The kinematical variables x_1 and x_2, $\hat{s}$=s$x_1 x_2$, and cos(θ^*)=tanh$\frac{|\eta_3 - \eta_4|}{2}$ can be calculated from the transverse momentum of the photon and the rapidities of the photon and the jet where η_3 and η_4, refer to the rapidities of the photon and the jet. f_g^A can then be extracted by a measurement of the cross section. Fig. 5, bottom-right shows the accuracy which can be reached in such a measurement in one run (here we have only taken into account a raw number of events - no detector effects have yet been folded in). Such measurements can then be used as direct inputs into models of heavy ion collisions.

5. Conclusions

In addition to the simulations mentioned here, the FOCAL group is now pursuing full simulations of transverse spin measurements, in particular to use γ-jet events to measure the Sivers effect, and to look at π^0s in jets to measure the Collins effect. We plan to have a proposal ready for review in the Fall of 2009. This will be followed by construction beginning in 2010 and installation in 2012.

References

1. DOE/NSF Nuclear Science Advisory Committee (2008), Report to NSAC of the Subcommittee on Performance Measures Report to NSAC of the Subcommittee on Compelling Research Opportunities, Aug 2008, http://www.sc.doe.gov/henp/np/nsac/docs/PerfMeasEvalFinal.pdf.
2. O. Chvala et al. (PHENIX Collaboration), Proc. 24th Winter Workshop on Nuclear Dynamics, EP Systema, Budapest (2008) 301-306. O. Chvala et al. (PHENIX Collaboration), Submitted to EPJ-C, doi:10.1140/epjc/s10052-009-0953-y (2009).
3. D. de Florian, R. Sassot, M. Stratmann and W. Vogelsang, Phys. Rev. Lett. **101**, 072001 (2008) [arXiv:0804.0422 [hep-ph]].
4. T. Gehrmann and W. J. Stirling, Phys. Rev. D **53**, 6100 (1996) [arXiv:hep-ph/9512406].
5. C. Nonaka, J. Phys. G **34**, S313 (2007) [arXiv:nucl-th/0702082].
6. K. J. Eskola, H. Paukkunen and C. A. Salgado, JHEP **0807**, 102 (2008) [arXiv:0802.0139 [hep-ph]].
7. H. Paukkunen, K. J. Eskola and C. A. Salgado, arXiv:0903.1956 [hep-ph].